ARTICLE IN PRESS

Available online at www.sciencedirect.com

ScienceDirect

Mathematics and Computers in Simulation ▮ (▮▮▮▮) ▮▮▮–▮▮▮

MATHEMATICS AND COMPUTERS IN SIMULATION

www.elsevier.com/locate/matcom

Original articles

Modelling and simulation of a robust energy efficient AUV controller

M. Sarkar[a,b,*], S. Nandy[b], S.R.K. Vadali[b], S. Roy[b], S.N. Shome[b]

[a] *Academy of Scientific & Innovative Research, CSIR-CMERI, Durgapur, India*
[b] *Robotics & Automation Division, CSIR-CMERI, Durgapur, India*

Received 24 July 2014; received in revised form 6 June 2015; accepted 30 August 2015

Abstract

Limited on-board energy resources of autonomous underwater vehicles (AUVs) demand design of an appropriate controller to achieve optimal energy consumption while tracking a commanded path accurately for some envisaged applications. The unstructured oceanic environment calls for a robust control law which is capable of handling parametric uncertainties and environmental disturbances. Though switching surface control has been proven to be an effective strategy for underwater operations, it provides no scope for energy optimization. For an energy critical mission, it is desirable to minimize the net control effort through advanced mathematical modelling, even at the cost of compromising accuracy within a reasonable bound. With this aspect in mind, the present work addresses these two issues (i.e. energy and accuracy) together through design of a novel controller based on sliding mode control in association with Euler–Lagrange based classical optimal control. Mathematical modelling and simulation results are presented to demonstrate the effectiveness of the proposed controller with real life parameters of an experimentally validated AUV, designed and developed for 150 m depth of operation at sea.

Keywords: Sliding mode control; Trajectory tracking; Optimal control; Euler–Lagrange equations

1. Introduction

Autonomous Underwater Vehicles (AUVs) are intelligent mobile robots capable of handling complicated tasks underwater. Two major challenges of autonomous underwater robotics are, (a) effective navigation of the robot in an unstructured and uncertain environment and (b) optimal utilization of limited on-board battery power for specific applications.

In general, power system of AUV relies on the on-board power supply. Although Zinc–Silver batteries provide double energy density over lead–acid, they are not cost effective like the former one as reported by Yuh [18]. Presently, AUV researchers are utilizing Li-polymer/Li-Ion batteries, which are the lightest and have highest energy density but they are relatively very costly. Thus there is a strong need to utilize the costly and mission dependent on-board

* Corresponding author at: Academy of Scientific & Innovative Research, CSIR-CMERI, Durgapur, India.
E-mail addresses: meenakshisarkar7@gmail.com (M. Sarkar), snandy@cmeri.res.in (S. Nandy), srk_vadali@cmeri.res.in (S.R.K. Vadali), sroy002@gmail.com (S. Roy), snshome@cmeri.res.in (S.N. Shome).

http://dx.doi.org/10.1016/j.matcom.2015.08.021
0378-4754/

Please cite this article in press as: M. Sarkar, et al., Modelling and simulation of a robust energy efficient AUV controller, Math. Comput. Simulation (2015), http://dx.doi.org/10.1016/j.matcom.2015.08.021

energy source of AUVs in an optimal manner while tracking a specified path with reasonable accuracy. This in turn addresses an active field of research on optimal control which is commonly achieved in association with optimal path planning [9], pertaining to AUV applications.

The inherent high nonlinearities and time-varying coupled dynamics of an autonomous underwater vehicle make the task of the control engineer highly challenging. Parametric uncertainties of hydrodynamic drag forces, variable centre of mass (COM) due to additional payload inclusion, highly unstructured and uncertain operating conditions and external disturbances (like ocean currents) contribute to the increase in complexities of the controller design. These additional complexities hinder the satisfactory performance of AUVs that use controllers based on traditional linear control theory. The inexact knowledge of hardware parameters of an AUV such as mass, centre of mass, inertia and centre of buoyancy, makes it difficult to implement conventional feedback linearization techniques, which further necessitates accurate sensory feedbacks,Vik & Fossen [15]. The inexact cancellation of nonlinearities, bounded parametric uncertainties, noisy sensory information and other environmental disturbances have inspired the researchers throughout the world to develop suitable control paradigm for underwater robotic systems.

Research purpose

The goal of the present work is to develop a mathematical framework for an energy efficient robust control algorithm that is capable of handling parametric as well as environmental disturbances. Many advanced control algorithms have already been proposed and explored by the researchers across the globe. Sliding mode control (SMC) by Yoerger and Slotine [17], Adaptive control by Fossen and Sagatum [6] and Cristi et al. [4], Adaptive learning control by Yuh [19], Backstepping and Lyapunov based technique by Lapierre [11], Robust outer loop control based on Lyapunov's second method by Roy et al. [13], are capable of handling the parametric and unstructured uncertainties on the system. Sliding mode control (SMC) reduces the complexity of the control problem by transferring an nth order system to one reduced order, while on the sliding surface. The finite time convergence condition and the property of insensitivity towards modelling imprecision make SMC a suitable candidate for underwater applications.

Chatchanayuenyong et al. [3] reported design of a time optimal sliding surface based on Pontryagin's Minimum Principle associated with neural networks but their model suffered from chattering effect due to high switching gains. Song et al. [14] tried to address similar time optimality problem with their rule based Fuzzy Sliding Mode controller. Smoothing the switching surface, in order to minimize the chattering effect, was attempted by Healey and Lienard [7] without leaving any scope for optimization. The linearized diving and steering plane controller based on second order sliding mode control as reported by Vuilmet [16] showed promising results for removing the high frequency chattering signals. Being inspired by nature, Barrett et al. [1] tried to address the optimization problem of flexible hull with genetic algorithms, while Kim and Ura [8] tried to arrive at a time optimal path planning solution with Euler–Lagrange formulations. Biggs and Holderbaum [2] weighted the quadratic cost function of their optimal kinematic controller to be equal to the instantaneous Lagrangian of the AUV. They investigated the necessary conditions for optimal motion along a helical path.

The inherent non-linearities of the AUV dynamics and parametric uncertainties make it extremely difficult in reaching an optimal solution in spite of utilizing modern optimization tools. Classical methods of solving Euler–Lagrange system leads to non-linear differential equations that pose the optimal solution in a time dependent open loop form rather than state dependent close-loop one. The convergence error of the optimal solution thus obtained for a two point boundary value problem (BVP) is highly dependent on the choice of the initial solutions. Although, the method proposed by Kim et al. [8] provides an effective means for generating best possible initial guess for a point to point guided navigation but it provides no scope for continuous trajectory tracking.

In the present work, we propose to address the robust trajectory tracking problem of AUV with effective energy utilization in two stages. Stage one consists of a switching surface based SMC, which addresses the robustness issues of the system against the modelling errors, uncertainties and environmental disturbances. In the second stage an Euler–Lagrange equation based energy optimal close-loop controller, that aims at minimizing the total control effort of the plant, is designed. The optimizer block searches the solutions in the immediate neighbourhood of the initial solutions provided by the sliding mode controller and thus generates the sub-optimal solutions. Since the proposed sub-optimal controller generates the final solutions based on the initial values provided by the SMC, it does not suffer from the convergence problem.

Please cite this article in press as: M. Sarkar, et al., Modelling and simulation of a robust energy efficient AUV controller, Math. Comput. Simulation (2015), http://dx.doi.org/10.1016/j.matcom.2015.08.021

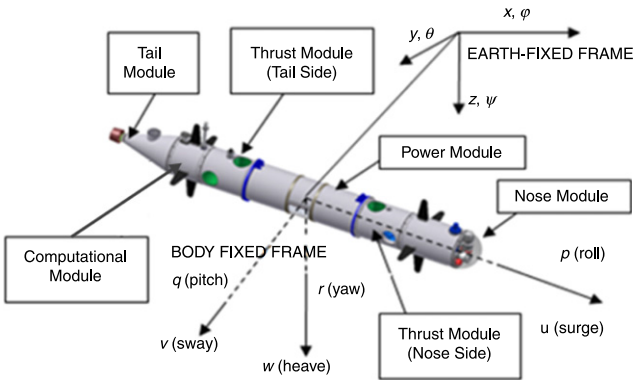

Fig. 1. Modular AUV-150 with reference frames and associated state directions.

2. Dynamics of an AUV

The complex AUV system, designed for 150 m depth under sea and christened as AUV-150, consists of many interconnected sub-systems comprising of mechanical, electrical, electronic, energy, propulsion, control and communication as well as other components and devices. All subsystems were designed concurrently to fulfil the overall design requirements of the AUV maintaining envisaged interrelationships. In opposition to the prevalent monolithic approach, the modular approach integrally associated with concurrent engineering paradigm has been followed. Modular construction provides the advantage of addition or removal of any payload or enhancement of energy system that might come into picture at subsequent stages of design accommodating minimal changes. However, modular construction in case of AUV-150 came with the added complexity of cable routing and networking between modules.

A torpedo shape of the vehicle is preferred to facilitate fabrication and a favourable length to diameter (L/D) ratio. Furthermore, the long and parallel modular mid-sections allow the vehicle length to be extended for future requirements. The vehicle (as shown in Fig. 1) comprises of a series of cylindrical hulls including a hemispherical frontal nose and a tapering tail section that can be quickly separated for vehicle reconfiguration, maintenance, and/or transportation. The design of AUV-150 was divided into six modules—(i) Nose module, (ii) Thrust module (nose-end), (iii) Power module, (iv) Thrust module (tail end), (v) Computational module and (vi) Tail module.

In the present work, kinematic and dynamic modelling of the AUV was carried out considering all forces acting on it while operating underwater. The equations of motion for six degrees of freedom autonomous underwater vehicle in body coordinate frame are given as [5]:

$$\mathbf{M}\dot{\mathbf{v}} + \mathbf{C}(\mathbf{v})\mathbf{v} + \mathbf{D}(\mathbf{v})\mathbf{v} + \mathbf{g}(\boldsymbol{\eta}) = \boldsymbol{\tau}, \tag{1}$$

where,

$$\begin{aligned}
&\mathbf{M}\epsilon\mathbb{R}^{6\times6} = \mathbf{M}_{RB} + \mathbf{M}_A,\\
&\mathbf{C}(\mathbf{v})\,\epsilon\,\mathbb{R}^{6\times6} = \mathbf{C}_{RB}(\mathbf{v}) + \mathbf{C}_A(\mathbf{v}),\\
&\mathbf{D}(\mathbf{v})\,\epsilon\,\mathbb{R}^{6\times6} = \mathbf{D}_L(\mathbf{v}) + \mathbf{D}_Q(\mathbf{v}),\\
&\boldsymbol{\eta}\,\epsilon\,\mathbb{R}^{6\times6} = \begin{bmatrix} x & y & z & \phi & \theta & \psi \end{bmatrix}^T,\\
&\mathbf{v}\,\epsilon\,\mathbb{R}^{6\times6} = \begin{bmatrix} u & v & w & p & q & r \end{bmatrix}^T.
\end{aligned}$$

$\mathbf{M}_{RB}$ and $\mathbf{M}_A$ represent the rigid body and added mass matrices, respectively. $\mathbf{C}_{RB}$ and $\mathbf{C}_A$ represents the rigid body and added Coriolis and centripetal matrices, respectively [5]. $\mathbf{D}_L$ and $\mathbf{D}_Q$ reflect the linear and quadratic drag matrices. The gravity and buoyancy force vector is represented by $\mathbf{g}(\boldsymbol{\eta})$ and vector $\boldsymbol{\tau}$ represents the input forces and moments. The linear positions and Euler angles expressed in inertial reference frame are denoted by $\boldsymbol{\eta}$, while $\mathbf{v}$ represents the linear and angular velocity vector expressed in body coordinate frame. Linear and angular velocities that are represented in both the frames are correlated by the kinematic transformation of the form:

$$\dot{\boldsymbol{\eta}} = \mathbf{J}(\boldsymbol{\eta})\mathbf{v}, \tag{2}$$

Please cite this article in press as: M. Sarkar, et al., Modelling and simulation of a robust energy efficient AUV controller, Math. Comput. Simulation (2015), http://dx.doi.org/10.1016/j.matcom.2015.08.021

where, $\mathbf{J}(\boldsymbol{\eta}) = \text{diag}\{\mathbf{J_1}(\boldsymbol{\eta}), \mathbf{J_2}(\boldsymbol{\eta})\}$ is the Jacobian matrix and the components related to the matrices $\mathbf{J_1}(\boldsymbol{\eta})$ and $\mathbf{J_2}(\boldsymbol{\eta})$ are detailed in [5]. The details of the parameters of AUV-150 which are considered for the present analysis are available in [13].

3. Design of Euler–Lagrange equation based energy sub-optimal sliding mode controller (SOSMC)

The proposed control law is divided into two stages as mentioned above, (i) Sliding Mode Control Block and (ii) Energy Sub-Optimizer Block. SMC is a form of variable structure control (VSC) that provides the necessary robustness for underwater operations. With appropriate construction of the sliding surfaces, the controller model remains uneffected by the modelling imperfections and external disturbances on the vehicle dynamics. The solutions generated by the switching control block are then fed to the optimizer block. At the next stage, the energy sub-optimizer block locally minimizes the net control effort of the system while compromising accuracy within a reasonably acceptable bound.

3.1. Design of sliding mode controller

Instead of defining the sliding surface in the domain of output error space [17], the sliding surfaces are designed in the state error space [7] with an objective of finding decoupled relationship for each of the control input. This methodology will guarantee state error convergence that will ensure stability and provide satisfactory performance. State errors pertaining to velocity and position of the vehicle are defined by:

$$\begin{bmatrix} \tilde{\mathbf{v}}(t) \\ \tilde{\boldsymbol{\eta}}(t) \end{bmatrix} = \begin{bmatrix} \mathbf{v}(t) - \mathbf{v_d} \\ \boldsymbol{\eta}(t) - \boldsymbol{\eta_d} \end{bmatrix}, \tag{3}$$

where, $\mathbf{v}(t)$ and $\boldsymbol{\eta}(t)$ are the velocity and posture vectors of the AUV system, respectively while, $\mathbf{v_d}$ and $\boldsymbol{\eta_d}$ correspond to desired values of velocity and position vectors, respectively. The sliding surfaces are defined in the error state space as:

$$\boldsymbol{\sigma}(\tilde{\mathbf{v}}, \tilde{\boldsymbol{\eta}}) = \mathbf{S^T} \begin{bmatrix} \tilde{\mathbf{v}}(\mathrm{t}) \\ \tilde{\boldsymbol{\eta}}(t) \end{bmatrix} = \begin{bmatrix} \mathbf{S}_1 & \mathbf{S}_2 \end{bmatrix} \begin{bmatrix} \mathbf{v}(t) - \mathbf{v_d} \\ \boldsymbol{\eta}(t) - \boldsymbol{\eta_d} \end{bmatrix}, \tag{4}$$

where, $\boldsymbol{\sigma}(t) \epsilon \mathbb{R}^{6\times 1}$; $\mathbf{S}_1, \mathbf{S}_2 \epsilon \mathbb{R}^{6\times 6}$.

The co-efficients of $\mathbf{S}_1, \mathbf{S}_2$ are taken to be known at this point. System error convergence rate will be affected with the choice of these two matrices. For closed-loop operation under feedback the system should fulfil,

$$\dot{\boldsymbol{\sigma}}(\tilde{\mathbf{v}}(t), \tilde{\boldsymbol{\eta}}(t)) \to \mathbf{0} \quad \text{as } t \to \infty, \tag{5}$$

subjected to,

$$\boldsymbol{\sigma}(\tilde{\mathbf{v}}(t), \tilde{\boldsymbol{\eta}}(t)) \to \mathbf{0} \quad \text{as } t \to \infty, \tag{6}$$

which implies,

$$\tilde{\mathbf{v}}(t) \to \mathbf{0}, \tilde{\boldsymbol{\eta}}(t) \to \mathbf{0} \quad \text{as } t \to \infty. \tag{7}$$

The global asymptotic stability of the system dynamics on the sliding surface is ensured from the definition of the Lyapunov function. $V(\boldsymbol{\sigma}(t))$ expressed in terms of $\boldsymbol{\sigma}(\tilde{\mathbf{v}}(t), \tilde{\boldsymbol{\eta}}(t))$ by,

$$V(\boldsymbol{\sigma}(t)) = \frac{1}{2}\boldsymbol{\sigma}^T(\tilde{\mathbf{v}}(t), \tilde{\boldsymbol{\eta}}(t))\boldsymbol{\sigma}(\tilde{\mathbf{v}}(t), \tilde{\boldsymbol{\eta}}(t)), \tag{8}$$

where, V is assumed as a positive definite and radially unbounded function. The global asymptotic stability would be assured if,

$$\frac{\mathrm{d}}{\mathrm{dt}} V(\boldsymbol{\sigma}) = \dot{\boldsymbol{\sigma}}^{\mathbf{T}}\boldsymbol{\sigma} < 0, \quad \forall \mathrm{t} > 0. \tag{9}$$

To satisfy this condition each $\sigma_i(t)$ is designed as:

$$\dot{\sigma}_i(\tilde{\mathbf{v}}(t), \tilde{\boldsymbol{\eta}}(t)) = -\lambda_i(t)\text{sgn}(\sigma_i(\tilde{\mathbf{v}}(t), \tilde{\boldsymbol{\eta}}(t))), \quad \text{for } i = 1, \ldots, 6 \tag{10}$$

where, $\lambda_i(t)$ is defined as a positive constant.

Please cite this article in press as: M. Sarkar, et al., Modelling and simulation of a robust energy efficient AUV controller, Math. Comput. Simulation (2015), http://dx.doi.org/10.1016/j.matcom.2015.08.021

But, this approach is not suitable for practical situations because of limited actuator bandwidth. One way of handling this situation is to replace the discontinuity with a smooth function [9]. To achieve this, we have defined the sliding surfaces mathematically by:

$$\dot{\sigma_i}(\tilde{\mathbf{v}}(t), \tilde{\boldsymbol{\eta}}(t)) = -\lambda_i(t)\frac{1-e^{-\gamma\sigma_i}}{1+e^{-\gamma\sigma_i}}, \tag{11}$$

where, $\gamma > 0, \forall t > 0$.

Differentiating (4) we get:

$$\dot{\boldsymbol{\sigma}} = \begin{bmatrix}\mathbf{S}_1 & \mathbf{S}_2\end{bmatrix}\begin{bmatrix}\dot{\mathbf{v}}(t) - \dot{\mathbf{v}_d} \\ \dot{\boldsymbol{\eta}}(t) - \dot{\boldsymbol{\eta}_d}\end{bmatrix}. \tag{12}$$

From the dynamics of AUV defined in Section 2 we have,

$$\dot{\boldsymbol{\sigma}} = \begin{bmatrix}\mathbf{S}_1 & \mathbf{S}_2\end{bmatrix}\begin{bmatrix}(-\mathbf{M}^{-1}\mathbf{C}(\mathbf{v})\mathbf{v} - \mathbf{M}^{-1}\mathbf{D}(\mathbf{v})\mathbf{v} - \\ \mathbf{M}^{-1}\mathbf{g}(\boldsymbol{\eta}) + \mathbf{M}^{-1}\mathbf{B}\mathbf{f}_{SMC} - \dot{\mathbf{v}}_d) \\ \mathbf{J}(\boldsymbol{\eta})\mathbf{v} - \dot{\boldsymbol{\eta}}_d\end{bmatrix} \tag{13}$$

where, $\boldsymbol{\tau} = \mathbf{B}\mathbf{f}_{SMC}$. $\mathbf{B}$ represents an equivalent mapping matrix and $\mathbf{f}_{SMC}$ denotes the vector of propeller forces. From (13) and (11) we get,

$$\begin{bmatrix}\mathbf{S}_1 & \mathbf{S}_2\end{bmatrix}\begin{bmatrix}(-\mathbf{M}^{-1}\mathbf{C}(\mathbf{v})\mathbf{v} - \mathbf{M}^{-1}\mathbf{D}(\mathbf{v})\mathbf{v} - \\ \mathbf{M}^{-1}\mathbf{g}(\boldsymbol{\eta}) + \mathbf{M}^{-1}\mathbf{B}\mathbf{f}_{SMC} - \dot{\mathbf{v}}_d) \\ \mathbf{J}(\boldsymbol{\eta})\mathbf{v} - \dot{\boldsymbol{\eta}_d}\end{bmatrix} = -\mathbf{F}(\boldsymbol{\sigma}), \tag{14}$$

where, $\mathbf{F}(\boldsymbol{\sigma}) \epsilon \mathbb{R}^{6\times 1}$ and $F_i(\sigma_i) = \lambda_i(t)\frac{1-e^{-\gamma\sigma_i}}{1+e^{-\gamma\sigma_i}}$.

Expanding (14) we get,

$$\begin{aligned}\Rightarrow -\mathbf{S}_1\mathbf{M}^{-1}\mathbf{C}(v)v - \mathbf{S}_1\mathbf{M}^{-1}\mathbf{D}(\mathbf{v})\mathbf{v} - \mathbf{S}_1\mathbf{M}^{-1}\mathbf{g}(\boldsymbol{\eta}) + \mathbf{S}_1\mathbf{M}^{-1}\mathbf{B}\mathbf{f}_{SMC} \\ - \mathbf{S}_1\dot{\mathbf{v}}_d + \mathbf{S}_2\mathbf{J}(\boldsymbol{\eta})\mathbf{v} - \mathbf{S}_2\dot{\boldsymbol{\eta}_d} \\ = -\mathbf{F}(\boldsymbol{\sigma})\end{aligned} \tag{15}$$

$$\Rightarrow \mathbf{f}_{SMC} = \mathbf{f}_1 + \mathbf{f}_2 + \mathbf{f}_3 \tag{16}$$

where,

$$\mathbf{f}_1 = (\mathbf{S}_1\mathbf{M}^{-1}\mathbf{B})^{-1}[\mathbf{S}_1\mathbf{M}^{-1}\mathbf{C}(\mathbf{v})\mathbf{v} + \mathbf{S}_1\mathbf{M}^{-1}\mathbf{D}(\mathbf{v})\mathbf{v} + \mathbf{S}_1\mathbf{M}^{-1}\mathbf{g}(\boldsymbol{\eta}) + \mathbf{S}_1\dot{\mathbf{v}}_d], \tag{17}$$

$$\mathbf{f}_2 = (\mathbf{S}_1\mathbf{M}^{-1}\mathbf{B})^{-1}[\mathbf{S}_2\dot{\boldsymbol{\eta}_d} - \mathbf{S}_2\mathbf{J}(\boldsymbol{\eta})\mathbf{v}], \tag{18}$$

$$\mathbf{f}_3 = -(\mathbf{S}_1\mathbf{M}^{-1}\mathbf{B})^{-1}\mathbf{F}(\boldsymbol{\sigma}). \tag{19}$$

The component $\mathbf{f}_1$ of the overall control which is given by (16) provides estimation of forces to perform the required manoeuvre, component $\mathbf{f}_2$ provides stabilization based on estimation of the positional elements and component $\mathbf{f}_3$ represents a switching term that drives the state errors to the sliding surface.

Eqs. (15) and (16) show that, the output of the SMC i.e., $\mathbf{f}_{\mathbf{SMC}}$ contains feed-forward, non-linear feedback and non-linear switching components that add inherent robustness into the system.

3.2. Mathematical framework for design of optimal control law

The performance index for the optimal control block is constructed with an objective of minimizing the total control effort for desired trajectory tracking. The cost function J is defined here as:

$$J = \frac{1}{2}\int_{t_0}^{t_f}\left\{(\mathbf{x}(t) - \mathbf{x}_d(t))^T\mathbf{Q}(\mathbf{x}(t) - \mathbf{x}_d(t)) + \mathbf{f}_{SMC}^T(t)\mathbf{U}\mathbf{f}_{SMC}(t)\right\}dt, \tag{20}$$

where, $\mathbf{x}(t) \epsilon \mathbb{R}^{12\times 1} = \begin{bmatrix}\mathbf{v} \\ \boldsymbol{\eta}\end{bmatrix}$, $\mathbf{x}_d(t) \epsilon \mathbb{R}^{12\times 1} = \begin{bmatrix}\mathbf{v}_d \\ \boldsymbol{\eta}_d\end{bmatrix}$. $\mathbf{Q} \epsilon \mathbb{R}^{12\times 12}$ and $\mathbf{U} \epsilon \mathbb{R}^{6\times 6}$, are two positive definitive matrices.

Please cite this article in press as: M. Sarkar, et al., Modelling and simulation of a robust energy efficient AUV controller, Math. Comput. Simulation (2015), http://dx.doi.org/10.1016/j.matcom.2015.08.021

It should be noted that, instead of constructing the cost function which minimizes the control effort in fractional degrees as reported by Kumar et al. [10], a quadratic approach similar to that of a Linear Quadratic Regulator (LQR) has been adopted here. Also, a feedback loop has been designed and implemented by adding the error terms in the performance index. Here, a trade off is required between the tracking error and minimum control effort by giving more weightage to either of them through choice of proper co-efficient for **U** and **Q** as the situation arises.

Subsequent incorporation of the dynamics of AUV into the cost function with Lagrange Multipliers gives us the augmented performance index which is given by:

$$J_a = \int_{t_0}^{t_f} \left\{ \begin{array}{c} \frac{1}{2}((\mathbf{x}(t) - \mathbf{x}_d(t))^T \mathbf{Q}(\mathbf{x}(t) - \mathbf{x}_d(t)) + \mathbf{f}_{SMC}^T(t)\mathbf{U}\mathbf{f}_{SMC}(t)) \\ + \begin{bmatrix} \mathbf{P}_1 & \mathbf{P}_2 \end{bmatrix} \begin{bmatrix} (-\mathbf{M}^{-1}\mathbf{C}(\mathbf{v})\mathbf{v} - \\ \mathbf{M}^{-1}\mathbf{D}_{\mathrm{mod}(\mathbf{v})\mathbf{v}} - \mathbf{M}^{-1}\mathbf{g}(\boldsymbol{\eta}) \\ + \mathbf{M}^{-1}\mathbf{B}\mathbf{f}_{SMC}) \\ \mathbf{J}(\boldsymbol{\eta})\mathbf{v} \end{bmatrix} \end{array} \right\} dt, \tag{21}$$

where, $\mathbf{P}_1, \mathbf{P}_2 \in \mathbb{R}^{6\times 6}$ are the matrices of Lagrange Multipliers and t_f and t_0 define the final and initial time values, respectively.

The modified equivalent drag-coefficient matrix is defined by $\mathbf{D}_{mod}$ and the parameters are evaluated according to:

$$\mathbf{D}_{mod}(\mathbf{v}) = \mathrm{diag} \left\{ \begin{array}{c} -120u\tanh(u), -1224v\tanh(v), -1224w\tanh(w), 0, \\ -2731q\tanh(q), -2731r\tanh(r) \end{array} \right\}.$$

The original drag-coefficient matrix **D** defined in [13], contained discontinuous terms which cause singularity while evaluating the Lagrange Multipliers. Those discontinuities have been removed in $\mathbf{D}_{mod}(\mathbf{v})$ with a hyperbolic (tangent) smoothing function. For optimal control problem, Hamiltonian has a special relevance.

From (21) the Hamiltonian is formulated as:

$$\begin{aligned} \mathbb{H}(\mathbf{x}(t), \mathbf{f}_{SMC}(t), \mathbf{P}(t), t) = {} & \frac{1}{2}\mathbf{f}_{SMC}^T(t)\mathbf{U}\mathbf{f}_{SMC}(t) + \frac{1}{2}(\mathbf{x}(t) - \mathbf{x}_d(t))^T\mathbf{Q}(\mathbf{x}(\mathbf{t}) - \mathbf{x}_d(t)) \\ & + \begin{bmatrix} \mathbf{P}_1 & \mathbf{P}_2 \end{bmatrix} \begin{bmatrix} (-\mathbf{M}^{-1}\mathbf{C}(\mathbf{v})\mathbf{v} - \mathbf{M}^{-1}\mathbf{D}_{\mathrm{mod}(\mathbf{v})\mathbf{v}} - \\ \mathbf{M}^{-1}\mathbf{g}(\boldsymbol{\eta}) + \mathbf{M}^{-1}\mathbf{B}\mathbf{f}_{SMC}) \\ \mathbf{J}(\boldsymbol{\eta})\mathbf{v} \end{bmatrix}. \end{aligned} \tag{22}$$

Using Euler–Lagrange Method of *variational calculus* we get the *state equations* as follows:

$$\dot{\mathbf{x}}^*(t) = \frac{\partial \mathbb{H}(\mathbf{x}^*(t), \mathbf{f}_{SMC}^*(t), \mathbf{P}^*(t), t)}{\partial \mathbf{P}}, \tag{23}$$

where, $\dot{\mathbf{x}}^*(t)$ defines the nominal trajectory and $\mathbf{f}_{SMC}^*(t)$ defines the nominal control law.

Co-state equations are defined by:

$$\dot{\mathbf{P}}^*(t) = \begin{bmatrix} \dot{\mathbf{P}}_1^* \\ \dot{\mathbf{P}}_2^* \end{bmatrix} = -\frac{\partial \mathbb{H}(\mathbf{x}^*(t), \mathbf{f}_{SMC}^*(t), \mathbf{P}^*(t), t)}{\partial \mathbf{x}}. \tag{24}$$

Now, using the steepest descent method, the steepest gradient of $\mathbb{H}$ is evaluated according to:

$$\Delta\mathbf{f} = \frac{\partial \mathbb{H}(\mathbf{x}^*(t), \mathbf{f}_{SMC}^*(t), \mathbf{P}^*(t), t)}{\partial \mathbf{f}_{SMC}}. \tag{25}$$

The system of differential equations (23)–(25) searches the entire neighbourhood to achieve the global optimum solution. In this endeavour the boundary conditions are defined by:

$$\mathbf{P}^*(t_f) = \mathbf{0}.$$

In our proposed method instead of searching the entire neighbourhood, we have tried to arrive at a local minimum by restricting our search in the immediate neighbourhood. The output of the SMC is now subsequently optimized by

Please cite this article in press as: M. Sarkar, et al., Modelling and simulation of a robust energy efficient AUV controller, Math. Comput. Simulation (2015), http://dx.doi.org/10.1016/j.matcom.2015.08.021

searching the immediate neighbourhood of radius δ_i as expressed by:

$$f_{SOSMC_i} = f_{SMC_i} - \delta_i \Delta f_{SOSMC_i}, \quad \text{for } i = 1, \ldots, 6 \tag{26}$$

where, $\delta_i \geqslant 0 \forall i$ and f_{SMC_i} constitutes the decoupled output from the SMC. f_{SOSMC_i} is the final output of the sub-optimal controller that is optimized in the direction of steepest descent. Constant diagonal matrix $\boldsymbol{\delta}$ acts as the deciding factor between tracking error and optimum control effort. For a small value of δ_i the corresponding search space for the sub-optimal solution will be very small which might not yield satisfactory optimal performance of the controller. Reasonable increase of δ_i will definitely increase the volume of the search-space, which in turn will improve the performance of the controller. Since the direction of the steepest descent is defined only in the immediate neighbourhood of f_{SMC_i}, unlimited increase of the volume of the search space leads to degradation of the error performance and stability of the system. Due to the presence of inherent non-linearity in the system of differential equations (23)–(25), the constant matrix $\boldsymbol{\delta}$ is highly problem specific and needs to be tuned accordingly.

4. Simulation studies and analysis

The real life parameters of AUV-150 as enlisted in [13] have been used to verify the proposed control law in simulated environment. The basic objective of AUV-150 is to survey deep water environment at sea. Various trajectories are targeted for verification and comparison purposes starting from simple depth control to composite path tracking (lawn mower). The main objective of the proposed control law is to make the system energy efficient through minimization of total control effort within an acceptable range of tracking error. A detailed structure of the Energy Sub-Optimal Sliding Mode Control (SOSMC) framework is presented in Fig. 2. A detailed comparative study between SMC [7] and the proposed Energy Sub-Optimal Sliding Mode control (SOSMC) is presented here through various illustrations. Parametric variations are taken into consideration for intensive mathematical simulation and are provided in Table 2.

The overall system mass is varied over time from the nominal mass (i.e. 490 kg) to the time-varying sinusoidal augmented mass (Fig. 3) to verify the performance of the controller with time-varying parametric uncertainties for any value within the predefined bounds. The robustness of the controller to imprecise modelling of the hydrodynamic coefficients as well as Coriolis components are also verified by changing the coefficients arbitrarily within the operating range of AUV-150.

4.1. Response to depth control along with surge and pitch

Trajectory definition for the depth manoeuvre with simultaneous activation of surge and pitch controller is defined according to:

$$X_d = 0.25t, \qquad Y_d = 0, \qquad Z_d = 0.09t, \qquad \phi_d = 0^\circ, \qquad \theta_d = 20^\circ, \qquad \psi_d = 0^\circ.$$

Controller parameters for SMC and the SOSMC for Depth control are taken as:

$$\mathbf{S}_1 = \text{diag}\{1, 1, 1, 1, 1, 1\}, \qquad \mathbf{S}_2 = \text{diag}\{1, 1, 1, 1, 1, 1\},$$
$$\boldsymbol{\lambda} = \text{diag}\{1, 1, 3, 1, 3, 1\}, \qquad \boldsymbol{\delta} = \text{diag}\{0.2, 0.3, 0.27, 0, 0.15, 0.01\}.$$

The parameters of $\mathbf{S}_1$ and $\mathbf{S}_2$ matrices are judiciously chosen from the state-error response of the system to ensure finite time reach ability to the sliding surface. The switching gain matrix $\boldsymbol{\lambda}$ is evaluated based on the bounds on the parametric uncertainties. The diagonal matrix $\boldsymbol{\delta}$ has been tuned to achieve a near optimal search space considering a judicious balance between accuracy and efficiency of the controller.

The percentage of improvement on total control effort is evaluated by the following mathematical framework:

$$\frac{\int_{t_0}^{t_f} \mathbf{f}_{SMC}^T \mathbf{f}_{SMC} dt - \int_{t_0}^{t_f} \mathbf{f}_{SOSMC}^T \mathbf{f}_{SOSMC} dt}{\int_{t_0}^{t_f} \mathbf{f}_{SMC}^T \mathbf{f}_{SMC} dt} \times 100\%. \tag{27}$$

Based on the above expression 21.75% improvement on total control effort is achieved with the proposed control law with respect to the conventional SMC [7] while achieving a depth up to 27 m which is achieved in 300 s, with

Please cite this article in press as: M. Sarkar, et al., Modelling and simulation of a robust energy efficient AUV controller, Math. Comput. Simulation (2015), http://dx.doi.org/10.1016/j.matcom.2015.08.021

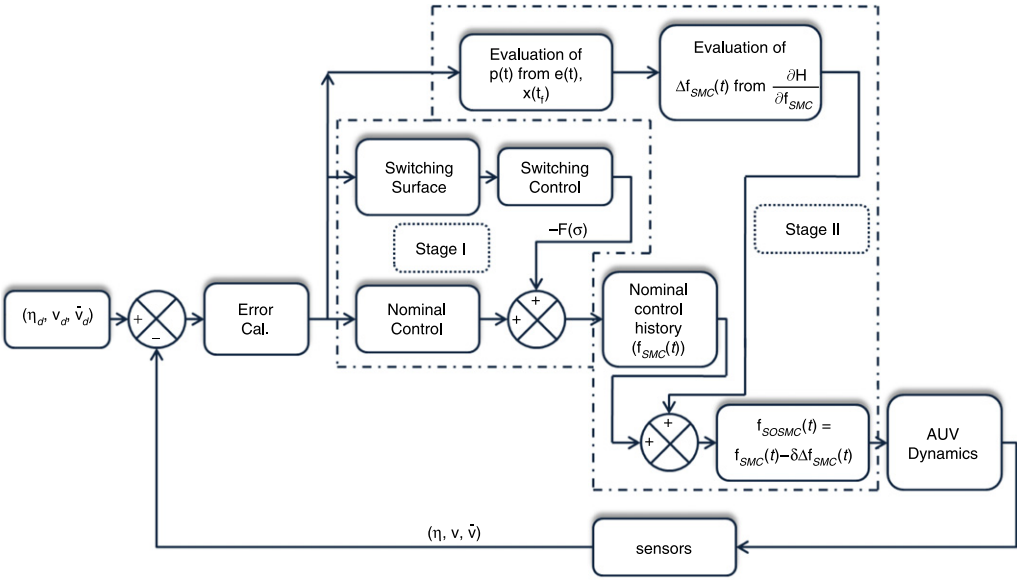

Fig. 2. Schematic framework of the proposed SOSMC.

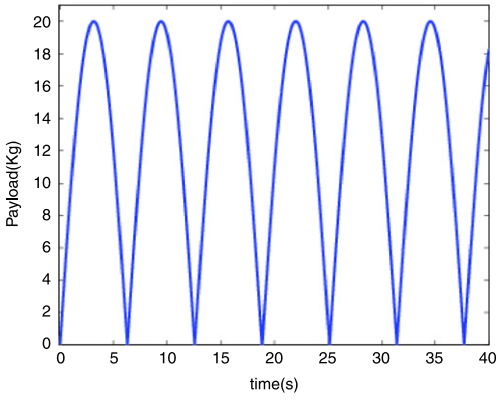

Fig. 3. $|Sinusoidal|$ payload variation.

effective forward velocity of 0.27 m s^{-1}. The average X-positional error for sliding mode is noted as 4.12 mm, where as for the proposed control law it turns out to be 8.35 mm as represented in Fig. 4(a). The improved efficiency of control effort as depicted in Fig. 5 came at the cost of a marginal compromise of the system's error performance.

4.2. Step response to heading (yaw) control

For Heading control, a step input of 30° is taken as reference for controlling yaw (ψ_d) where as the reference signals for controlling the rest of the 5 degrees of motion are taken as:

$$X_d = 0.25t, \qquad Y_d = 0.144t, \qquad Z_d = 0, \qquad \phi_d = 0°, \qquad \theta_d = 0°.$$

The parameters for both SMC and SOSMC for Heading control are selected as:

$$\mathbf{S}_1 = \text{diag}\{1, 1, 1, 1, 1, 1\}, \qquad \mathbf{S}_2 = \text{diag}\{1, 1, 1, 1, 1, 1\},$$

$$\boldsymbol{\lambda} = \text{diag}\{1, 1, 8, 1, 3, 1\},$$

$$\boldsymbol{\delta} = \text{diag}\{0.2, 0.3, 0.27, 0, 0.1, 0.1\}.$$

Please cite this article in press as: M. Sarkar, et al., Modelling and simulation of a robust energy efficient AUV controller, Math. Comput. Simulation (2015), http://dx.doi.org/10.1016/j.matcom.2015.08.021

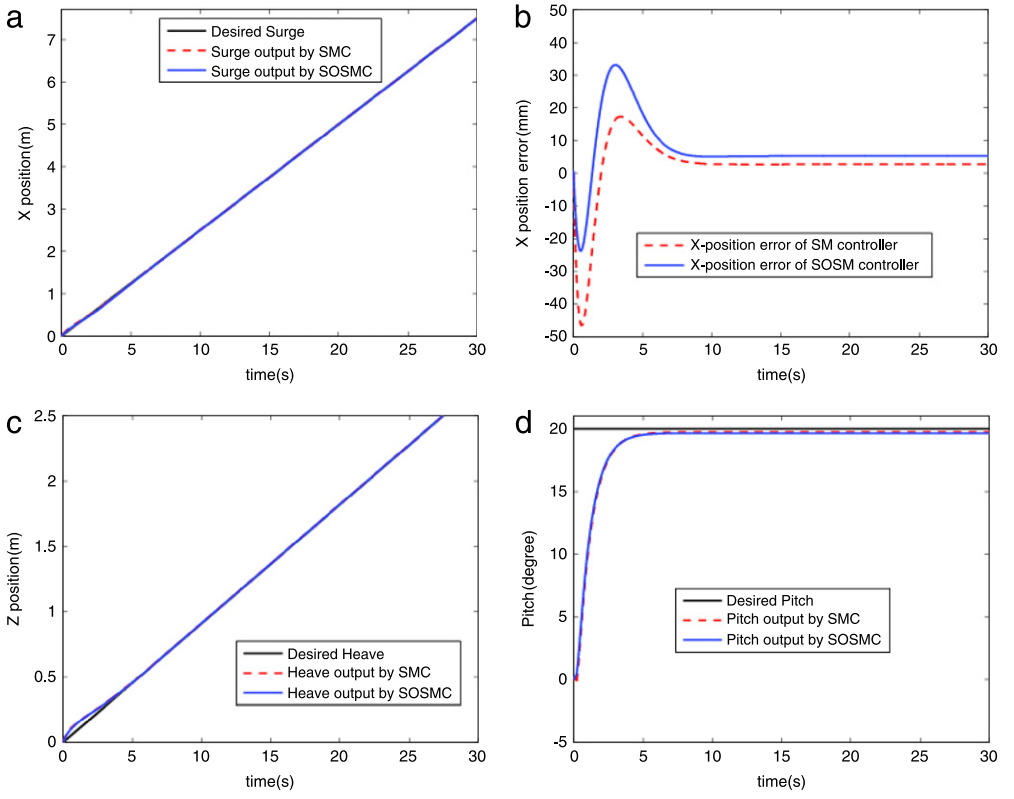

Fig. 4. Comparative study between the desired trajectory (black line) and the output trajectories realized by SMC (red line) and SOSMC (blue line) for (a) Surge, (c) Heave and (d) Pitch for controlling depth. (b) shows a comparative study of X-positional error plots between SMC and SOSMC. (For interpretation of the references to colour in this figure legend, the reader is referred to the web version of this article.)

Based on the mathematical expression given in (27), 22.27% savings of total control effort has been noticed for controlling the heading of the vehicle with simultaneous activation of surge and sway from (0 m, 0 m, 0^0) to (7.5 m, 4.32 m, 30^0). The improved efficiency can be easily identified from the comparative study of the control effort plots given in Fig. 7(a)–(c). Fig. 6(a)–(c) give idea about the transient and steady state performance of the controller to the desired input reference where as Fig. 6(d) shows that SOSMC generates more promising transient error response than SMC [7].

4.3. Composite trajectory tracking (lawn mower)

Since the basic purpose of AUV-150 is to survey the deep sea environment, a lawn mower trajectory has been simulated to verify the performance of the proposed controller. Lawn mower path is mainly used for sea-bed mapping during survey missions.

According to Roy et al. [12] so far the lawn mower path has been expressed intuitively as a mixture of sinusoid and square wave. In the simulated environment, at first the vehicle is commanded to achieve a depth of 50 m with a completely decoupled depth controller. Then the AUV is instructed to follow the desired lawn mower path in the X–Y plane. The envisaged Lawn Mower path (25 m × 15 m) is selected by:

$$X_d = 2.5\sin(0.1t) + 0.25t, \qquad Y_d = 12.5\cos(0.05t), \qquad Z_d = 50, \qquad \phi_d = 0^\circ, \qquad \theta_d = 0^\circ,$$

$$\psi_d = \frac{1}{20\pi}\sum_{n=1}^{n=\infty}\left(\left(\frac{64\pi^2}{5n} - \frac{40\pi}{n}\sin\left(\frac{n\pi}{10}\right) - \frac{32\pi}{n^2}\cos\left(\frac{n\pi}{10}\right)\right)\right) \times \sin\left(\frac{n\pi}{2}\right)\sin\left(\frac{nt}{20}\right)^\circ.$$

Please cite this article in press as: M. Sarkar, et al., Modelling and simulation of a robust energy efficient AUV controller, Math. Comput. Simulation (2015), http://dx.doi.org/10.1016/j.matcom.2015.08.021

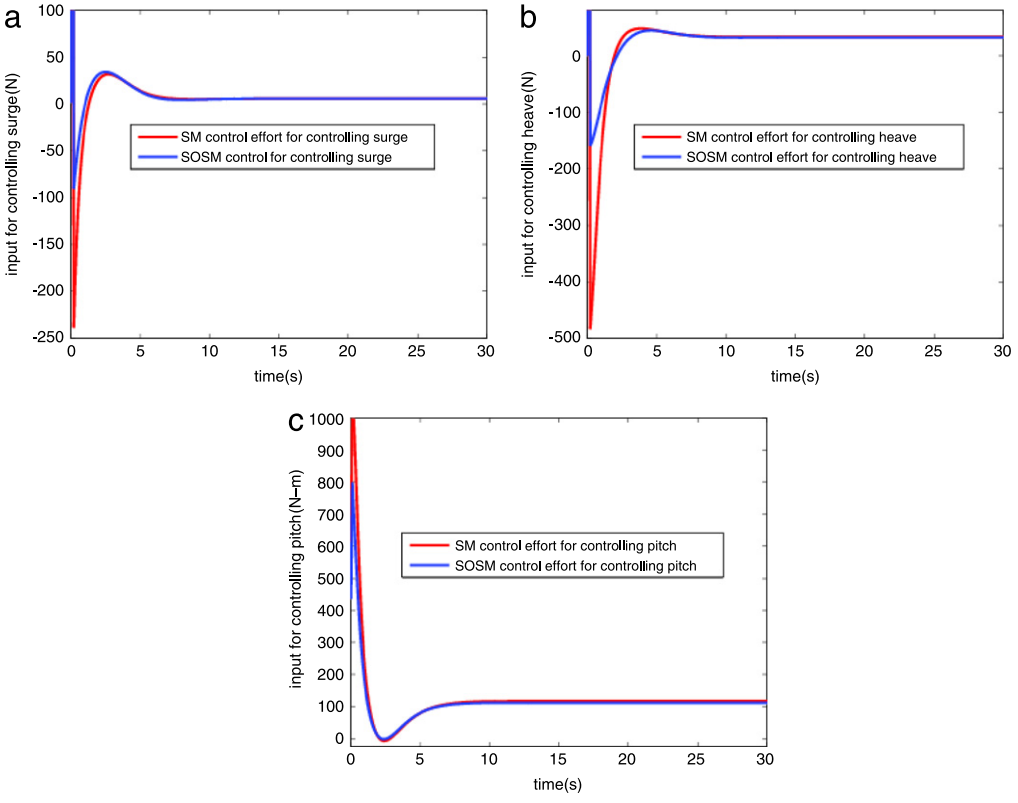

Fig. 5. Comparative study of (a) Surge, (b) Heave, (c) Pitch control effort by SMC (red line) and SOSMC (blue line) for controlling depth. (For interpretation of the references to colour in this figure legend, the reader is referred to the web version of this article.)

Table 1
Performance comparison of SMC and SOSMC for lawn mower path.

Error		Lawn Mower (25 × 15)		Lawn Mower (20 × 10)		Lawn Mower (30 × 20)	
		SMC	SOSMC	SMC	SOSMC	SMC	SOSMC
Max error	e_{path} (mm)	241	131.8	204.1	94.48	267.6	105.6
	e_{ψ}	1.37°	1.33°	1.17°	1.03°	1.98°	1.30°
Avg error	e_{path} (mm)	18.67	32.86	14.92	36.25	23.62	55.0
	e_{ψ}	0.19°	0.19°	0.22°	0.23°	0.35°	0.36°
%Improved efficiency		14.70%		15.03%		7.3%	

Desired lawn mower path and the corresponding heading (Yaw) information are depicted in Fig. 8(a) and (b), respectively. Controller design parameters for the lawn mower path are taken as:

$$\mathbf{S}_1 = \text{diag}\{1, 1, 1, 1, 1, 1\}, \qquad \mathbf{S}_2 = \text{diag}\{1, 1, 1, 1, 1, 1\},$$
$$\boldsymbol{\lambda} = \text{diag}\{1, 1.5, 1, 1, 2.5, 3\},$$
$$\boldsymbol{\delta} = \text{diag}\{0.2, 0.15, 0.1, 0, 0.01, 0.01\}.$$

It is clearly visible from the control effort plots (Fig. 10(a)–(c)) that the proposed control law minimizes the net control effort of the system. Although this improved efficiency comes at the cost of accuracy within an acceptable bound (Fig. 9(a), (b)). Based on the expression given by (27), 14.70% relative improvement of the net control effort has been observed while tracking a lawn mower path for around 200 s. A detailed comparative study of the proposed control law, with respect to energy saving, for various dimensions of lawn mower path has been provided in Table 1. It is observed that the improved performance of the proposed control law (SOSMC), in terms of energy savings and tracking error, is more prominent during the transient phase (Fig. 10(d)).

Please cite this article in press as: M. Sarkar, et al., Modelling and simulation of a robust energy efficient AUV controller, Math. Comput. Simulation (2015), http://dx.doi.org/10.1016/j.matcom.2015.08.021

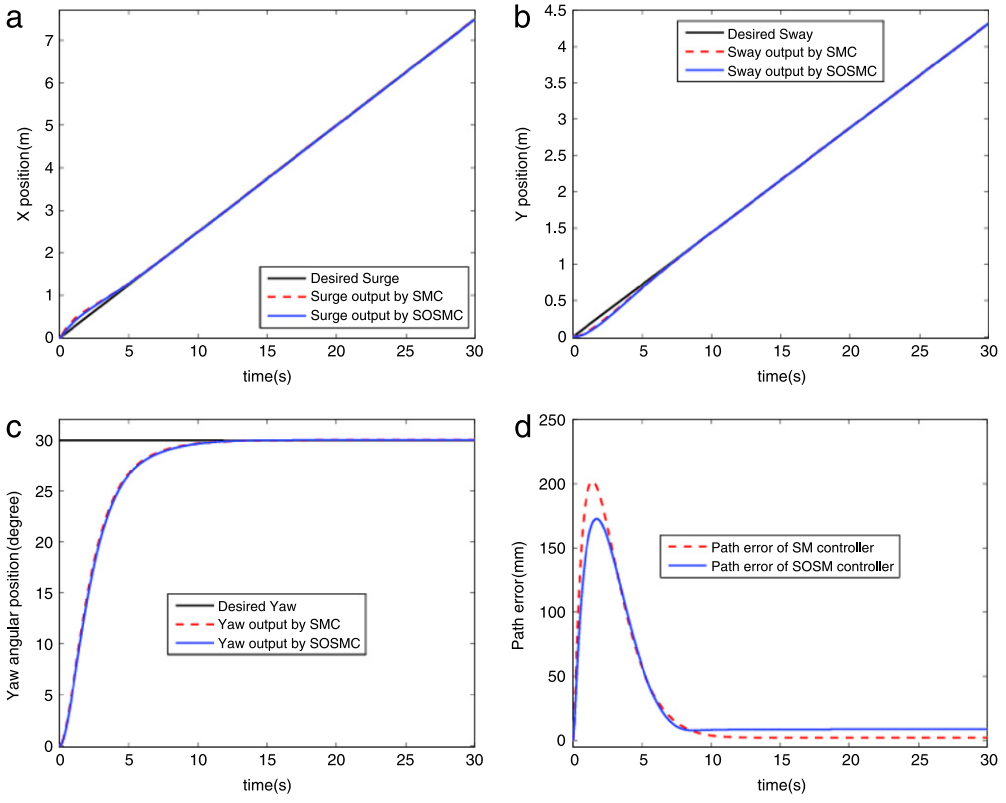

Fig. 6. Comparative study between the desired output (black line) and the output by SMC (red line) and SOSMC (blue line) for (a) Surge, (b) Sway and (c) Yaw for the desired Heading. (d) shows a comparative study of Path error plots between SMC and SOSMC. (For interpretation of the references to colour in this figure legend, the reader is referred to the web version of this article.)

Table 2
Values of nominal parameters and their deviations.

	m (kg)	x_G (m)	y_G (m)	z_G (m)	I_x (kg m^2)	I_y (kg m^2)	I_z (kg m^2)	$-X_{\dot{u}}$	$-Y_{\dot{v}}$
NV[a]	490	0	0	0.012	17.1	632	630	49	836
PD[b]	20e[c]	0.08e	0.003e	0.015e	1.6e	4e	7e	.6e	10e

[a] NV = Nominal Values.
[b] PD = Parametric Deviation.
[c] $e = |20\sin(t)|$. The parametric nomenclature and units are taken as [5].

5. Conclusion

Autonomous underwater vehicles are important tools for deep oceanic explorations as well as various mission specific applications. We have presented here a detailed mathematical framework for an energy sub-optimal robust control (SOSMC) algorithm for AUV, working in an unstructured deep sea environment, pertinent to the efficient use of on-board energy supplied through batteries.

We have focused our research on the SMC, one of the well established and widely used robust control methodologies. Although, SMC is well tested for parametric uncertainties it does not provide any scope for energy optimization. The proposed control law provides a novel approach, through judicious combination of ordinary SMC and classical optimal control paradigm, to find a feasible sub-optimal energy solution while tracking various commanded path. Performance of the novel controller is verified through rigorous numerical simulation and promising results are noted. Substantial savings of energy, as observed from the illustrations of SOSMC, will definitely help to increase the AUV mission duration to a greater extent.

Please cite this article in press as: M. Sarkar, et al., Modelling and simulation of a robust energy efficient AUV controller, Math. Comput. Simulation (2015), http://dx.doi.org/10.1016/j.matcom.2015.08.021

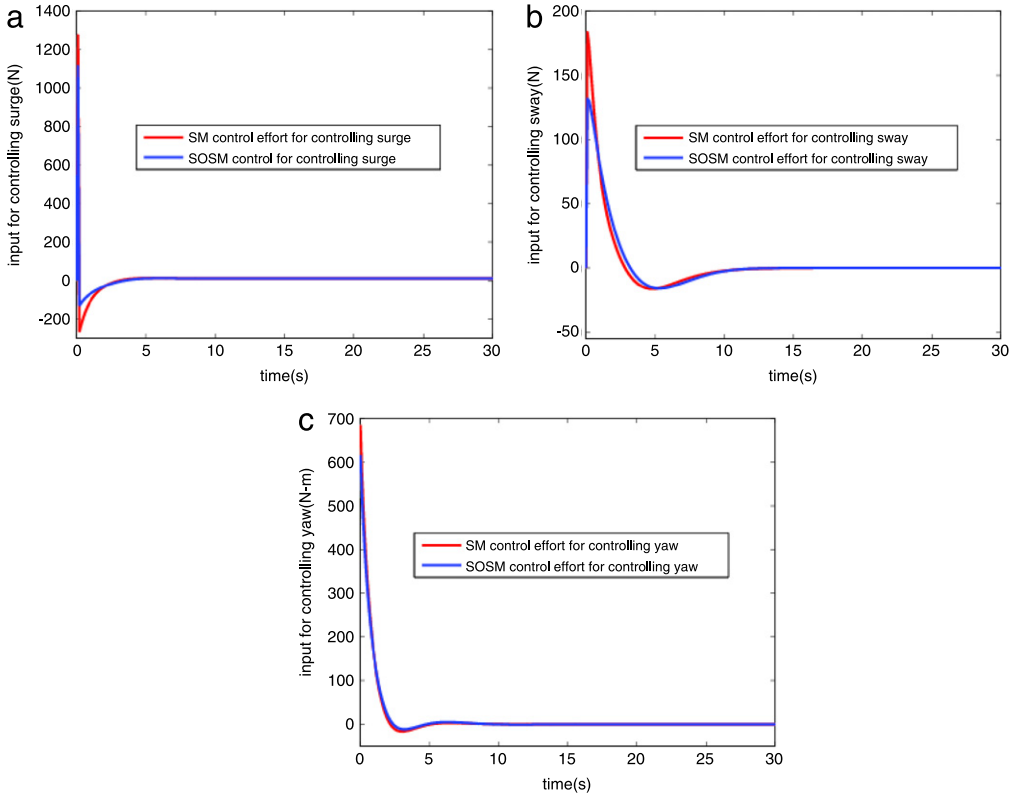

Fig. 7. Comparative study of (a) Surge, (b) Sway, (c) Yaw control efforts realized by SMC (red line) and SOSMC (blue line) for controlling heading from (0 m, 0 m, 0°) to (7.5 m, 4.32 m, 30°). (For interpretation of the references to colour in this figure legend, the reader is referred to the web version of this article.)

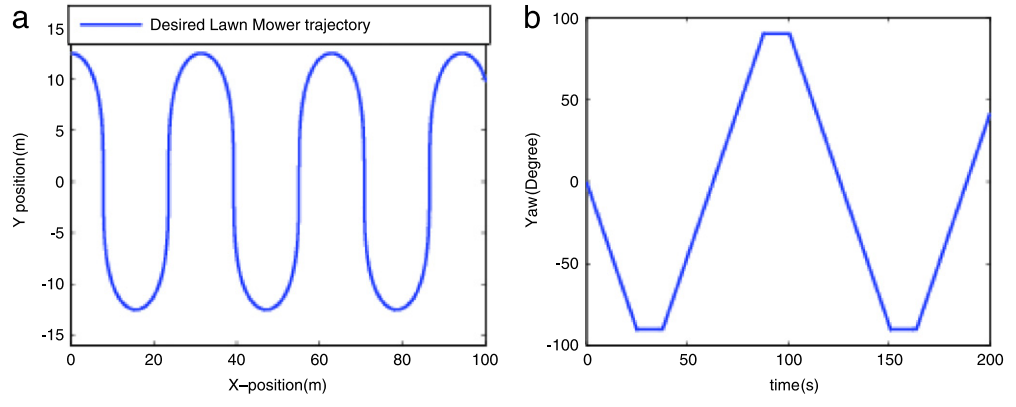

Fig. 8. (a) The desired trajectory of Lawn Mower path in the X–Y plane and (b) corresponding yaw.

Acknowledgements

The authors of this research article are grateful to all the members of Robotics and Automation Group, CSIR-CMERI who are directly or indirectly involved in design and development of AUV-150. The authors also gratefully acknowledge the sponsor of this project, Ministry of Earth Sciences (MoES), Government of India. The results of this research work would be applied for UnWaR (ESC-0113) project in due course of time.

Please cite this article in press as: M. Sarkar, et al., Modelling and simulation of a robust energy efficient AUV controller, Math. Comput. Simulation (2015), http://dx.doi.org/10.1016/j.matcom.2015.08.021

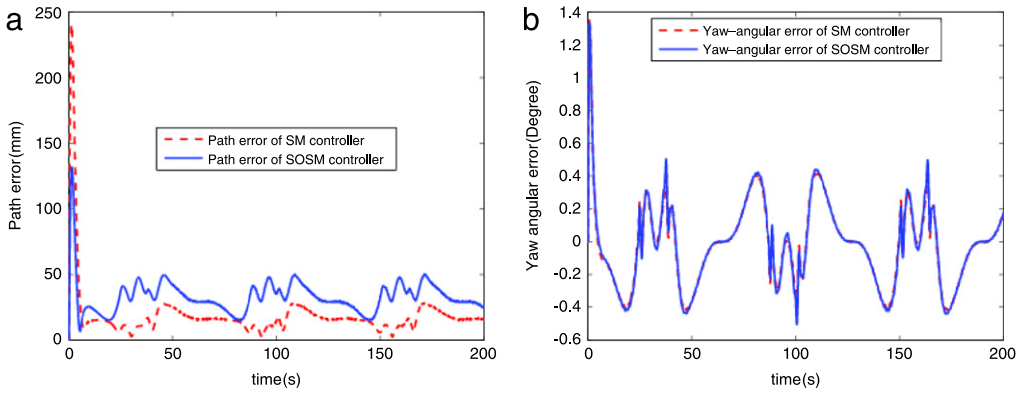

Fig. 9. Comparison of (a) Path error, (b) Yaw angular error for Lawn Mower path realized by SMC (red line) and SOSMC (blue line). (For interpretation of the references to colour in this figure legend, the reader is referred to the web version of this article.)

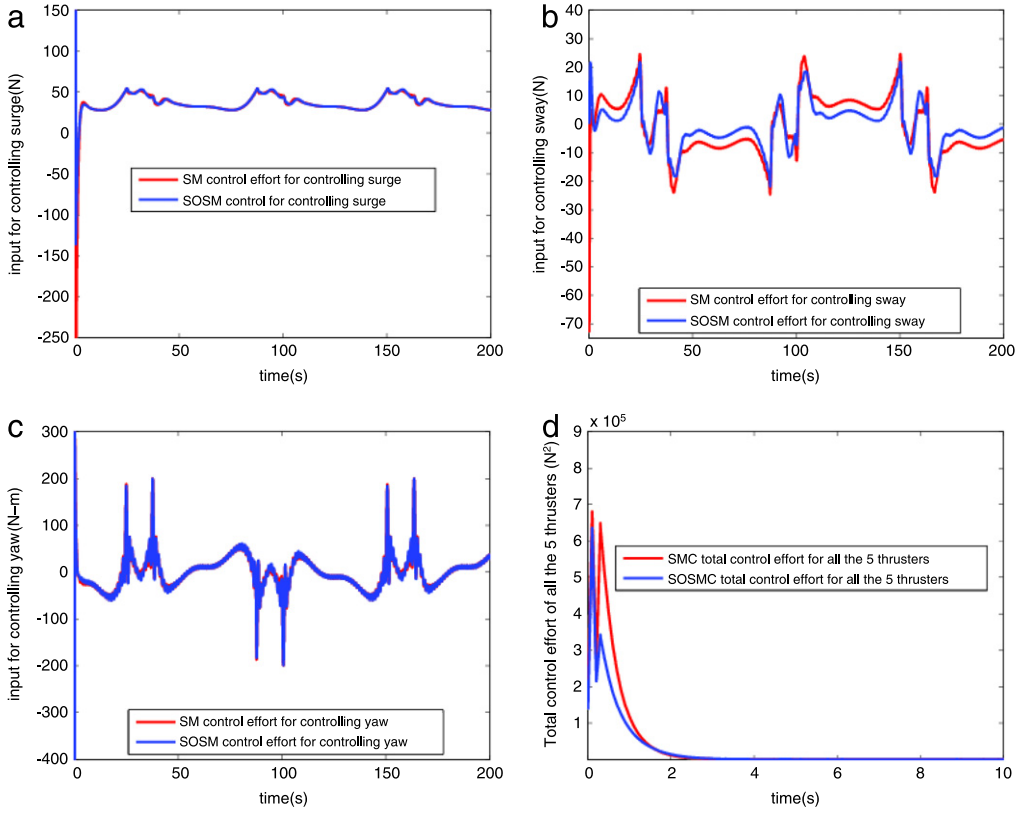

Fig. 10. Comparative study of (a) Surge, (b) Sway, (c) Yaw control effort realized by SMC (red line) and SOSMC (blue line) for controlling AUV-150 along a lawn mower path. (d) shows the comparison between the total transient control effort of SMC (red line) and SOSMC (blue line) while tracking Lawn Mower path. (For interpretation of the references to colour in this figure legend, the reader is referred to the web version of this article.)

References

[1] D. Barrett, M. Grosenbaugh, M. Triantafyllou, The optimal control of a flexible hull robotic undersea vehicle propelled by an oscillating foil, in: Proc. Symp. Autonomous Underwater Vehicle Technology, AUV'96, Monterey, CA, USA, 1996, pp. 1–9.

[2] J. Biggs, W. Holderbaum, Optimal kinematic control of an autonomous underwater vehicle, IEEE Trans. Autom. Control 54 (2009) 1623–1626.

Please cite this article in press as: M. Sarkar, et al., Modelling and simulation of a robust energy efficient AUV controller, Math. Comput. Simulation (2015), http://dx.doi.org/10.1016/j.matcom.2015.08.021

[3] T. Chatchanayuenyong, M. Parnichkun, Neural network based-time optimal sliding mode control for an autonomous underwater robot, Mechatronics 16 (2006) 471–478.
[4] R. Christi, F.A. Papoulias, A.J. Healey, Adaptive sliding mode control of autonomous underwater vehicles in the dive plane, IEEE J. Ocean. Eng. 15 (1990) 152–160.
[5] T.I. Fossen, Guidance and Control of Ocean Vehicles, first ed., John Wiley & Sons, Chichester, 1994.
[6] T.I. Fossen, S. Sagatun, Adaptive control of nonlinear systems: a case study of underwater robotic systems, J. Robot. Syst. 8 (1991) 393–412.
[7] A.J. Healey, D. Lienard, Multivariable sliding mode control for autonomous diving and steering of unmanned underwater vehicles, IEEE J. Ocean. Eng. 18 (1993) 327–339.
[8] K. Kim, T. Ura, Optimal and quasi-optimal navigations of an AUV in current disturbances, in: Proc. IEEE/RSJ Int. Conf. Intelligent Robots and Systems IROS, Nice, France, 2008, pp. 3661–3667.
[9] D. Kruger, R. Stolkin, A. Blum, J. Briganti, Optimal AUV path planning for extended missions in complex, fast-flowing estuarine environments, in: Proc. IEEE Int. Conf. Robotics and Automation, ICRA, Roma, Italy, 2007, pp. 4265–4270.
[10] R.P. Kumar, A. Dasgupta, C.S. Kumar, Real-time optimal motion planning for autonomous underwater vehicles, Ocean Eng. 32 (2005) 1431–1447.
[11] L. Lapierre, Robust diving control of an AUV, IEEE J. Ocean. Eng. 36 (2008) 92–104.
[12] S. Roy, S. Nandy, S. Shome, R. Ray, Robust position control of an autonomous underwater vehicle: a comparative study, in: Proc. IEEE Int. Conf. Automation Science and Engineering, CASE, Madison, USA, 2013, pp. 1002–1007.
[13] S. Roy, S. Shome, S. Nandy, R. Ray, V. Kumar, Trajectory following control of AUV: a robust approach, J. Inst. Eng. (India): Ser. C 94.3 (2013) 253–265.
[14] F. Song, E. An, S.M. Smith, Design robust nonlinear controllers for autonomous underwater vehicles with comparison of simulated and at-sea test data, J. Vib. Control 8 (2002) 189–217.
[15] B. Vik, T.I. Fossen, A nonlinear observer for GPS and INS integration, in: Proc. 40th IEEE Conf. Decision and Control, CDC, vol. 3, Orlando, Florida, 2001, pp. 2956–2961.
[16] C. Vuilmet, High order sliding mode control applied to a heavyweight torpedo, in: Proc. IEEE Conf. Control Application, CCA, Toronto, Canada, 2005, pp. 61–66.
[17] D.R. Yoeger, J.J.E. Slotine, Robust trajectory control of underwater vehicles, IEEE J. Ocean. Eng. 10 (1985) 462–470.
[18] J. Yuh, Design and control of autonomous underwater robots: a survey, Auton. Robots 8 (2000) 7–24.
[19] J. Yuh, Learning control for underwater robotic vehicles, IEEE Control Syst. Mag. 8 (1994) 39–46.

Please cite this article in press as: M. Sarkar, et al., Modelling and simulation of a robust energy efficient AUV controller, Math. Comput. Simulation (2015), http://dx.doi.org/10.1016/j.matcom.2015.08.021